Quantum Electronics **51** (11) 970–975 (2021)

LASERS

https://doi.org/10.1070/QEL17638

Increasing the pump current range of a single-frequency laser diode tuned to the caesium D_2 line

O.O. Bagaeva, A.V. Ivanov, V.N. Drozdovskii, V.D. Kurnosov, K.V. Kurnosov, V.I. Romantsevich, V.A. Simakov, R.V. Chernov

Abstract. **It is shown experimentally and theoretically that increasing the pump current of a laser diode and simultaneously lowering its temperature can ensure an order of magnitude increase in the range of pump currents where the diode emission frequency is tuned to the caesium D_2 line. The results are compared to the case where the laser diode and fibre Bragg grating temperatures are maintained constant and only the laser pump current is varied.**

Keywords: *tunable single-frequency laser, fibre Bragg grating, spectral and power characteristics, tuning to the caesium D_2 line.*

1. Introduction

The development of laser emitters intended for use as highly stable resonant light sources for pumping and detecting a standard quantum transition in quantum frequency standards (QFS's) based on atomic caesium (^{133}Cs) and rubidium (^{87}Rb) beams and vapour helps further improve performance characteristics of GPS and GLONASS global navigation satellite systems.

The greatest promise for use in atomic-beam tubes (ABTs) is offered by single-frequency laser diodes (LDs), which have a small size and weight, are easy to pump, and ensure high efficiency of electrical energy conversion to coherent light in the wavelength range 850–895 nm, covering the region of resonant optical transitions in caesium atoms.

A great deal of attention is currently paid to the development of single-frequency lasers (including those operating in the range 1.3–1.6 μm) for transmitting large volumes of information. Bagaeva et al. [1] demonstrated a high-power single-frequency ridge laser (200 mW, mesa stripe width of 3 μm, side-mode suppression ratio from 30 to 50 dB) with a sidewall first-order diffraction grating, operating at wavelengths from 1.5 to 1.6 μm. The distributed feedback (DFB) laser fabrication process usually comprises two cycles: heterostructure (HS) growth and Bragg grating inscription. To complete the fabrication of the laser device structure, it is necessary to cap the open grating surface with a semiconductor material via epitaxial growth. The process involves a number of technological difficulties, resulting in defect formation.

O.O. Bagaeva, A.V. Ivanov, V.N. Drozdovskii, V.D. Kurnosov, K.V. Kurnosov, V.I. Romantsevich, V.A. Simakov, R.V. Chernov
OJSC M.F. Stel'makh Polyus Research Institute, ul. Vvedenskogo 3/1, 117342 Moscow, Russia; e-mail: KurnosovKV@niipolyus.ru

Received 19 July 2021
Kvantovaya Elektronika **51** (11) 970–975 (2021)
Translated by O.M. Tsarev

The above-mentioned drawbacks can be avoided by using a longitudinal Bragg grating located on both sides of the active region and optically coupled to it. The diffraction grating was produced using electron-beam lithography at the Institute of Microwave Semiconductor Electronics, Russian Academy of Sciences, and the HS was grown, the active element was produced, the device was assembled, and its parameters were determined at OJSC M.F. Stel'makh Polyus Research Institute. The technology can be utilised for making a single-frequency laser emitting at a wavelength of 852 nm.

In this work, an emitter design based on a diffraction grating in single-mode optical fibre is proposed for obtaining single-frequency LD operation [2]. The emitter wavelength can then be varied by changing not only the LD temperature and pump current but also the temperature of the fibre Bragg grating (FBG), which allows the emitter wavelength to be fine-tuned to ultrafine transitions of caesium atoms.

Zhuravleva et al. [3] presented a calculational model for an external-cavity FBG LD and showed that, in their model, single-frequency lasing could be obtained with no allowance for spectral hole burning. They experimentally determined the ranges of LD currents and temperatures and Bragg grating temperatures in which the laser could be tuned to the caesium D_2 line.

Spectral characteristics of an emitter with a Bragg grating soldered onto a thermoelectric cooler (TEC) were studied experimentally and theoretically by Ivanov et al. [4]. They described a model for the emitter with allowance for the pressure resulting from the soldering of the Bragg grating onto the thermoelectric cooler, as well as for the temperature and dispersion. Their theoretical results were in satisfactory agreement with their experimental data.

Threshold, power, and spectral characteristics of an FBG emitter were studied experimentally and theoretically by Zholnerov et al. [5]. Their results demonstrate that it is important to take into account heating of the active region of the LD, its thermal resistance, and the cavity output power because this allows one to adequately explain the discontinuities observed in power and spectral characteristics.

They also studied power and spectral characteristics of an FBG LD at various fibre lengths and thermal resistances of the diode [6]. They obtained a simplified relation for the gain coefficient of the LD.

For the operation of a QFS, it is necessary to use an automatic system for maintaining the laser emitter frequency (wavelength). The broader is the range of pump currents in which the laser frequency can be tuned to the caesium D_2 line, the more reliable is the automatic frequency tuning system. In this paper, we propose an approach for extending the pump

current range of a laser diode emitter based on a diffraction grating inscribed in single-mode optical fibre. The block diagram of a fibre Bragg grating laser and optimisation of its parameters were reported elsewhere [7–9]. Issues pertaining to the use of single-frequency lasers were addressed by Fang et al. [10]. The use of optical methods in ABTs allows magnetic selection of atoms according to their state to be replaced by more effective methods: optical pumping and optical detection. This simplifies the geometry and design of the instrument, reduces its weight, considerably improves the efficiency of the utilisation of the working substance, and increases the output signal amplitude [3].

In this work, we demonstrate that, if the LD pump current is increased and, simultaneously, the LD temperature is lowered, the range of pump currents in which the emission wavelength corresponds to tuning to the caesium D_2 line can be extended by an order of magnitude. First, we consider the case where the LD and FBG temperatures are maintained constant and study spectral and power characteristics of the emitter at a varied pump current. Next, these characteristics are analysed and compared at a constant FBG temperature and varied LD temperature. Calculated spectral and power characteristics are shown to be in satisfactory agreement with experimental data.

2. Experimental

Figure 1 shows a schematic of the fibre Bragg grating laser emitter. In our experiments, we used MOVPE-grown GaAs/AlGaAs-based LDs with a 90-Å-thick active region. To the left and right of the active region, there were 0.12-μm-thick waveguide layers and 1.5-μm-thick emitter layers. The LD length was 1200 μm. The laser diode face opposite the objective had a protective coating, and the other face, opposite the FBG, had an anti-reflection coating with a reflectivity under 0.5%. The LDs were soldered, with their active region up, onto a contact plate, which was in turn soldered onto a TEC. Next, the FBG-containing metallised fibre was aligned and fixed relative to the active region of the LD. The fibre was secured to another TEC. The refractive index period of the FBG was chosen so as to obtain lasing at a wavelength of 852 nm.

Spectral and power characteristics of the laser output were measured with a setup schematised in Fig. 2. During the measurements, the emitter (*4*) was enclosed in an external thermostat. The LD beam was directed through beam splitter cubes (*7*, *8*) to the inputs of an optical spectrum analyser (*9*) (Yokogawa AQ6319), saturation spectroscopy module (*10*) (TEM-Messtechnik CoSy), and scanning confocal interferometer (*12*) (interferometer response function, 1.5 MHz; free spectral range, 250 MHz). The laser output was sent to the optical spectrum analyser through a collimator and a fibre segment (omitted in Fig. 2). The signal from the saturation spectroscopy module was recorded on oscilloscope *11*, and the signal from the interferometer, on oscilloscope *13*.

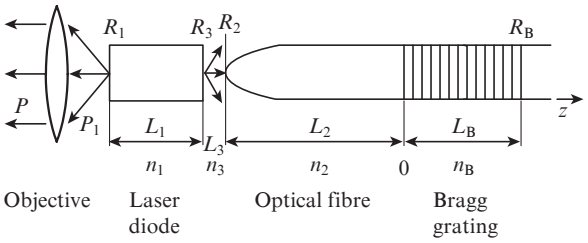

Figure 1. Schematic of the fibre Bragg grating semiconductor laser: L_1, n_1, L_2, n_2, L_3, n_3, L_B, and n_B are the lengths and refractive indices of the semiconductor laser, optical fibre, air gap, and Bragg grating; R_1, R_2, R_3, and R_4 are the corresponding reflectivities.

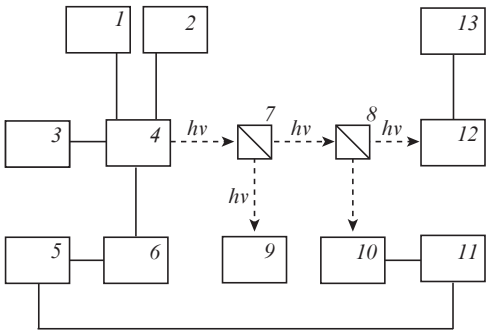

Figure 2. Block diagram of the devices used to check tuning to the caesium D_2 line:
(*1*, *2*) temperature controllers; (*3*) multimeter; (*4*) emitter placed in an external thermostat; (*5*) generator; (*6*) SRS LDC500 drive current controller; (*7*, *8*) beam splitter cubes; (*9*) Yokogawa AQ6319 optical spectrum analyser; (*10*) TEM-Messtechnik CoSy saturation spectroscopy module; (*11*, *13*) oscilloscopes; (*12*) scanning confocal interferometer.

During the measurements, the temperature in the external thermostat, which was used to reduce the effect of the ambient temperature on the LD, was maintained at 23.0 °C. LD and FBG thermal stabilisation conditions were ensured by temperature controllers (*1*, *2*). The LD pump current was provided by a dc controller (*6*) (SRS LDC500). In addition, a triangle-modulated current with a frequency of 10 Hz and an amplitude from 3 to 5 mA peak was superimposed on the direct pump current with the use of a generator (*5*) in order to ensure a slight wavelength sweep. When the emitter was tuned to the caesium D_2 line, six transitions were observed on the display of oscilloscope *11*, connected to the saturation spectroscopy module (*10*), which corresponded to the fine structure of caesium atoms (see also Ref. [11], Fig. 15). Concurrently, the triangular sweep current signal was shown in the centre of the display of oscilloscope *11*. By varying the pump current and LD temperature, the peak corresponding to the $4' - 5'$ transition (which was chosen as the best defined among others and located near the peak emission wavelength of the caesium D_2 line) was also located at the centre of the oscilloscope display (Fig. 3). Thus, as the sweep signal was reduced to zero, the constant LD pump current provided by the current controller (*6*) corresponded to the tuning of the emitter to the $4' - 5'$ transition.

Laser output parameters were measured in two steps. In the first step, only the LD pump current was varied during the measurements, whereas the LD and FBG temperatures were maintained constant. In the second step, the LD temperature and pump current were varied simultaneously, whereas the FBG temperature was constant.

At the beginning of the measurements, the emitter frequency was tuned to the D_2 line using controllers *1*, *2*, and *6* (varying the LD and FBG temperatures and LD pump current), and transitions corresponding to this line were observed on the display of oscilloscope *11*. After tuning the emitter to

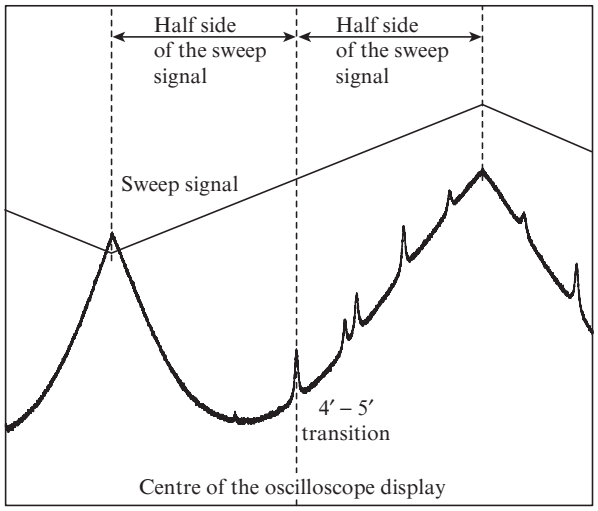

Figure 3. Transitions of the caesium D_2 line on the oscilloscope display.

the D_2 line, the LD and FBG temperatures were maintained constant and the LD pump current was increased and decreased relative to its value at the emitter frequency tuned to the D_2 line. In doing so, we measured the emission wavelength and power (the power meter is omitted in Fig. 2). Concurrently, single-frequency lasing was ascertained using the scanning interferometer. The laser output was thought to be single-frequency if single peaks were observed on the display of oscilloscope *13*, without any side components. When the optical power and laser wavelength were measured and single-frequency lasing was ascertained, the LD pump current was not modulated.

Figure 4 shows the emitter output power and wavelength as functions of pump current at constant LD and FBG temperatures. The pump current corresponding to point A is 47.9 mA, and that corresponding to point B is 67 mA, i.e. the pump current varies over 19.1 mA. In this range of pump currents, one external cavity mode was observed. Increasing the pump current after point B caused switching to another LD mode. The hatched region indicates the range of pump currents corresponding to multifrequency lasing (note that, at any pump current within the hatched region, single-frequency lasing can be obtained by properly adjusting the LD and FBG temperatures).

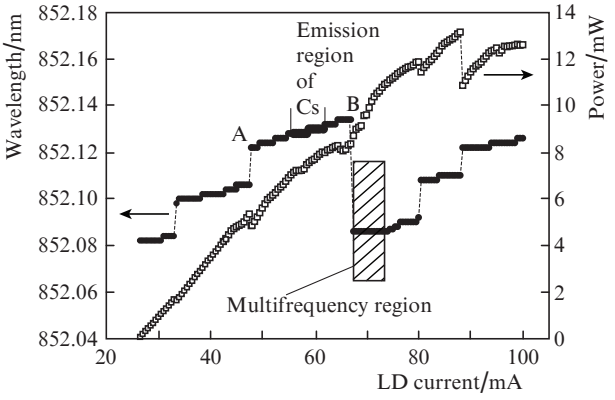

Figure 4. Emitter output power and emission wavelength as functions of pump current at constant LD and FBG temperatures.

It is also worth noting that the small wavelength steps between points A and B in Fig. 4 are due to the insufficient resolution of the Yokogawa AQ6319 optical spectrum analyser, while the wavelength varies continuously between these points (the resolving power of the analyser is 0.01 nm).

Figure 4 indicates the range of pump currents corresponding to emission from atomic caesium vapour. The width of this range is 5.7 mA (from 56 to 61.7 mA). Thus, at given LD and FBG temperatures, it is impossible to obtain emission from atomic caesium vapour in some part of the range A–B by varying only the pump current: it is necessary to vary the LD or FBG temperature as well.

Subsequently, we measured laser output parameters while simultaneously varying the pump current and LD temperature at a constant FBG temperature. The emitter was again tuned to the D_2 line using data obtained in the first step. On the display of oscilloscope *11*, we observed six transitions corresponding to the fine structure of caesium atoms and the triangular sweep current signal set symmetrically with respect to the centre of the display. A change in pump current or LD temperature leads to a change in laser emission wavelength, thus shifting peaks on the oscilloscope display. By varying the pump current and LD temperature, the peak corresponding to the $4' - 5'$ transition was brought in the centre of the display (Fig. 3). Thus, as the sweep current was reduced to zero, the LD pump current corresponded to the tuning of the emitter to the $4' - 5'$ transition. The corresponding pump current of the LD and resistance of a control thermistor that was soldered onto the contact plate near the LD and monitored its temperature were recorded [the resistance of the thermistor was measured by a multimeter (*3*), see Fig. 2].

In our measurements, the LD pump current was increased or decreased by about 1 mA, which shifted the $4' - 5'$ transition to one side or the other from the centre of the oscilloscope display, but a subsequent change in LD temperature again brought the peak to the centre. The new values of the pump current and the resistance of the control thermistor of the LD were also recorded. The maximum LD pump current (100 mA) was determined by the SRS LDC500 controller. As in the first step, single-frequency lasing was ascertained using the scanning interferometer (*12*).

As the current was reduced to below 36 mA, lasing was observed to switch to another longitudinal mode of the external cavity. In view of this, subsequent wavelength and output power measurements were made at points calculated by extrapolating previously obtained experimental data. The resistance of the control thermistor (R_{ct}) was calculated using the dependence on the pump current (I) given below.

The experimental data obtained as a result of the measurements in the second step are presented in Figs 5 and 6. Figure 5 shows the output power and wavelength as functions of pump current for the pump current and LD temperature varied simultaneously. For all data points at pump currents in the range 36–100 mA, the emission wavelength corresponds to the $4' - 5'$ transition. Moreover, the LD output was single-frequency at pump currents in the range 30–100 mA.

Figure 6 shows the measured resistance of the control thermistor of the LD as a function of pump current and a best-fit curve. The data points at pump currents in the range 36–100 mA were obtained at the emitter wavelength tuned to the $4' - 5'$ transition. The experimental data obtained in this range of pump currents are well fitted by the following polynomial:

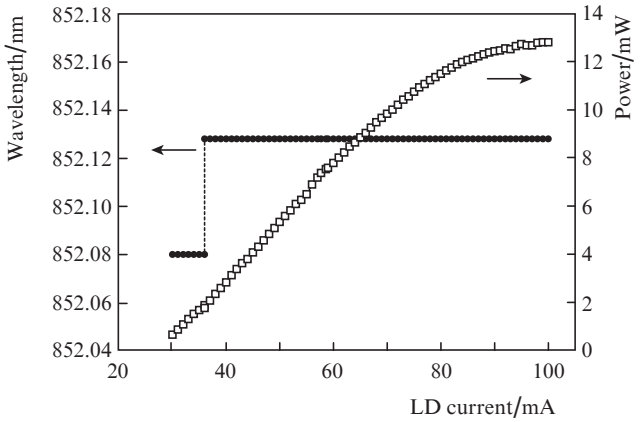

Figure 5. Emitter output power and emission wavelength as functions of pump current at a constant FBG temperature and simultaneously varied LD temperature.

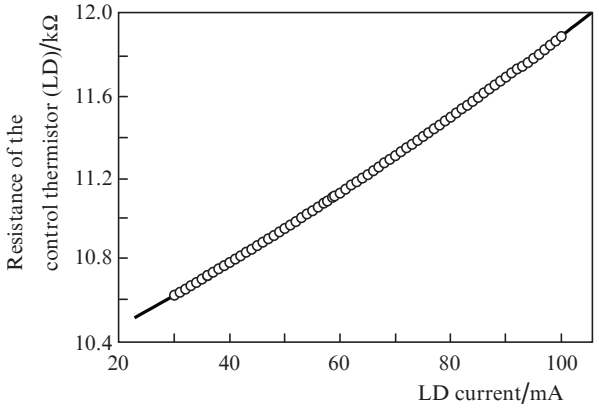

Figure 6. Measured resistance of the control thermistor of the LD as a function of pump current (open circles) and a best-fit curve (solid line).

$$R_{ct}(I) = 10.189 + 0.0132I + 4.311 \times 10^{-5} I^2 - 4.047 \times 10^{-8} I^3. \quad (1)$$

At pump currents below 36 mA, where the emitter could not be tuned to the $4' - 5'$ transition because of the change in its wavelength, R_{ct} was calculated using this relation. Note that the last two terms in (1) can be neglected to give a linear relation between R_{ct} and I, which is so in most cases according to the present experimental data.

The experimental data in Fig. 5 were obtained at R_{ct} varied in the range 10.6–11.9 kΩ (Fig. 6). The change in LD temperature in response to such changes in R_{ct} can be estimated using the relation

$$T_i = \frac{\beta}{\beta/T_0 - \ln(R_0/R_{cti})}, \quad (2)$$

where R_0 = 10 kΩ at a temperature T_0 = (273 + 25) K; β = 3970 K; and i = 1 or 2. Therefore, to the resistance R_{ct1} = 10.6 kΩ there corresponds a temperature T_1 = 296.70 K, and to R_{ct2} = 11.9 kΩ there corresponds T_2 = 294.16 K. It is seen that, in obtaining the experimental data in Fig. 5, the LD temperature changed by $T_1 - T_2$ = 2.54 °C.

Thus, producing a feedback system ensuring the variation in the resistance of the control thermistor according to (1), we will obtain a constant emission wavelength corresponding to the $4' - 5'$ transition at pump currents in the range 36–100 mA. Note that, whereas the range of pump currents in which emission from caesium vapour was observed at constant LD and FBG temperatures was 5.7 mA, here the range of pump currents in which the emission wavelength corresponds to the $4' - 5'$ transition is an order of magnitude broader: 64 mA.

3. Theory

The ability to produce an emitter tuned to a given wavelength and having the widest possible range of pump currents without switching to a neighbouring mode is a key issue in designing automatic emission frequency tuning systems. The calculations below demonstrate that the range of pump currents in which tuning to a given emission wavelength is possible can be extended by simultaneously increasing the LD current and reducing its temperature.

In our calculations, we rely on previously reported results [4–6]. The gain coefficient can be written in the form [6]

$$g_i = \frac{dg}{dn_a}[n_a D_i - n_{a0}(I)], \quad (3)$$

where $D_i = 1 - [2(E_i - E_g)/\Delta E_g]^2$; $E_i = 1.24/\lambda_i$ is the photon energy; λ_i (μm) is the emission wavelength of the ith mode; ΔE_g is the width of the gain spectrum; n_a is the carrier density in the active region of the LD; $n_{a0}(I) = a + bI$ is the carrier density at which the gain coefficient is zero; $a = 2.17 \times 10^{18}$ cm^{-3}; and $b = -1.67 \times 10^{16}$ cm^{-3} mA^{-1}.

The band gap E_g is given by

$$E_g = E_0 - 5.4 \times 10^{-4} \frac{T^2}{204 + T} - 2k_g n_a^{1/3}, \quad (4)$$

where E_0 = 1.63 eV; the factor 2 in the last term takes into account that there are equal electron and hole densities ($n_a = p_a$); and $k_g = 2 \times 10^{-8}$ eV cm. The temperature of the active region of the LD can be written in the form

$$T_{LD}(I, P_1) = T_0 + \delta T(I, P_1) + T_{ref}(I), \quad (5)$$

where

$$\delta T(I, P_1) = R_T(V_{pn} I \times 10^{-3} + (I \times 10^{-3})^2 R_g - 2P_1 \times 10^{-3}) \quad (6)$$

is the heating of the active region due to the pump current I passing through the LD and the optical power P_1 extracted from the LD cavity; R_T is the thermal resistance of the LD; V_{pn} is the voltage across the p–n junction; and R_g is the dynamic resistance of the LD. The additional change (reduction) in the heating of the LD can be represented in the form

$$T_{ref}(I) = fI \times 10^{-3}, \quad (7)$$

where f is the proportionality coefficient between the additional change in LD temperature and the pump current.

The optical power at the LD cavity output with reflectivity R_1 [3–6] is

$$P_1 = h\nu \frac{c_0}{n_{1gr}} A_c (1 - R_1) \sum_i S_{1i}, \tag{8}$$

where A_c is the cross-sectional area of the active region of the laser; c_0 is the speed of light in vacuum; S_{1i} is the average photon density in the LD cavity, given by (8) in Ref. [4]; and n_{1gr} is the group index. The optical power P at the output of the objective of the emitter is taken to be $0.8P_1$.

The pump current of the emitter can be represented in the form

$$I = I_{th} + qV_a \frac{c_0}{n_{1gr}} \sum_i \Gamma_a g_i S_{1i}, \tag{9}$$

where V_a is the volume of the LD active region; I_{th} is the threshold current; Γ_a is the optical confinement factor; and q is the electron charge.

If we are interested in the effect of the pump current on the spectral characteristics of the laser at a constant temperature of the contact plate below the LD (T_0) and a constant FBG temperature, the refractive index of the LD can be represented as

$$n_1(T_{LD}) = n_{10}\left\{1 + \frac{1}{n_{10}}\frac{\partial n_1}{\partial \lambda}(\lambda - \lambda_B) + \frac{1}{n_{10}}\left[\frac{\partial n_1}{\partial T_{LD}} + \Gamma_a \frac{\partial n_1}{\partial n_a}\frac{\partial n_a}{\partial T_{LD}}\right](T_{LD} - T_0)\right\}, \tag{10}$$

where n_{10} is the refractive index of the LD at $T_{LD} = T_0$ and $\lambda = \lambda_B$ (Bragg wavelength); $\partial n_1/\partial n_a$ is the change in the refractive index of the LD in response to a change in carrier density in the active region of the laser; and $\partial n_a/\partial T_{LD}$ is the change in carrier density in response to a change in the temperature of the LD active region.

The refractive indices of the FBG and fibre are taken in the form

$$n_B(\lambda) = n_{B0}\left[1 + \frac{1}{n_{B0}}\frac{\partial n_B}{\partial \lambda}(\lambda - \lambda_B)\right], \tag{11}$$

$$n_2(\lambda) = n_{20}\left[1 + \frac{1}{n_{20}}\frac{\partial n_2}{\partial \lambda}(\lambda - \lambda_B)\right], \tag{12}$$

where n_{B0} and n_{20} are the refractive indices of the FBG and fibre at $\lambda = \lambda_B$. The refractive index of the air gap is $n_3 = 1$. The LD length varies with temperature as

$$L_1(T_{LD}) = L_1(T_0)[1 + \alpha_T(T_{LD} - T_0)], \tag{13}$$

where α_T is the linear thermal expansion coefficient of the LD.

The following values were used in our calculations: $\Gamma_a = 9.6 \times 10^{-3}$, $L_1 = 0.12$ cm, $L_2 = 0.76$ cm, $L_3 = 30$ μm, $L_B = 1.0$ cm (see Fig. 1), $n_{10} = 3.3$, $n_{20} = n_{B0} = 1.452$, $n_3 = 1$, $R_1 = 0.3$, $R_2 = 0.04$, $R_3 = 0.005$, $R_B = 0.04$, $\partial n_1/\partial \lambda = -3 \times 10^3$ cm^{-1}, $\partial n_2/\partial \lambda = \partial n_B/\partial \lambda = -160$ cm^{-1}, $n_{10}^{-1}[\partial n_1/\partial T + \Gamma_a(\partial n_1/\partial n_a) \times (\partial n_a/\partial T)] = 0.77 \times 10^{-4}$, $R_g = 5$ Ω, $V_{pn} = 1.46$ V, $R_T = 18$ K W^{-1}.

Figure 7 shows the LD output power and emission wavelength as functions of pump current at $f = 0$, constant LD and FBG temperatures, and a coupling coefficient of counterpropagating waves $K_0 = 6$ cm^{-1} [5]. Comparison of Figs 4 and 7 demonstrates satisfactory agreement between the calculation results and experimental data.

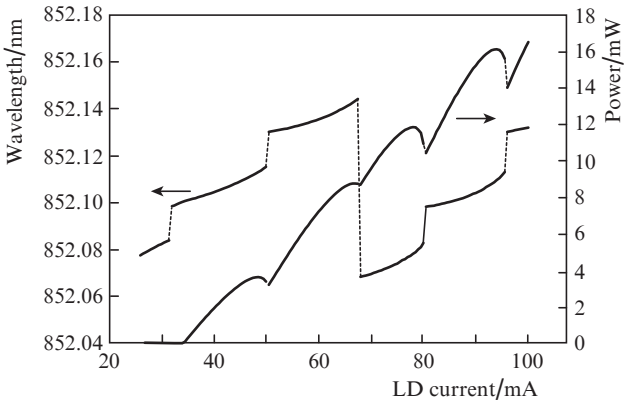

Figure 7. LD output power and emission wavelength as functions of pump current at $f = 0$.

Figure 8 shows the emitter output power and wavelength as functions of pump current at $f = -25.5$ K A^{-1}, constant FBG temperature, and the LD temperature varied according to relation (5) at the same f and $K_0 = 6$ cm^{-1}. The data in Figs 5 and 8 are also in satisfactory agreement. The calculation results suggest that, at a pump current of 100 mA, the additional decrease in the heating of the LD according to (7) is 2.55 °C, which correlates with the 2.54 °C obtained above.

Thus, it has been shown that the range of pump currents in which the emission wavelength corresponds to the $4' - 5'$ transition of the caesium D_2 line can be extended by an order of magnitude by increasing the pump current of the laser diode and simultaneously lowering its temperature. Such a procedure for controlling the emitter wavelength ensures an

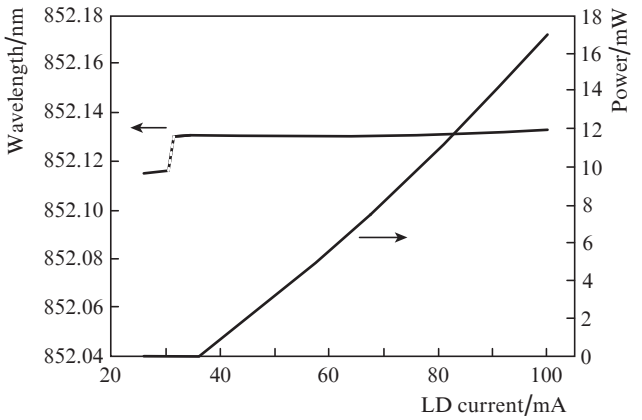

Figure 8. LD output power and emission wavelength as functions of pump current at $f = -25.5$ K A^{-1}.

order of magnitude broader range of LD pump currents than in the case where the laser diode and Bragg grating temperatures are maintained constant. The calculation results have been shown to be in satisfactory agreement with the present experimental data.

References

1. Bagaeva O.O., Galiev R.R., Danilov A.I., et al. *Quantum Electron*., **50**, 143 (2020) [*Kvantovaya Elektron*., **50**, 143 (2020)].
2. Zhuravleva O.V., Ivanov A.V., Leonovich A.I., Kurnosov V.D., Kurnosov K.V., Chernov R.V., Shishkov V.V., Pleshanov S.A. *Quantum Electron*., **36**, 741 (2006) [*Kvantovaya Elektron*., **36**, 741 (2006)].
3. Zhuravleva O.V., Ivanov A.V., Kurnosov V.D., Kurnosov K.V., Mustafin I.R., Simakov V.A., Chernov R.V., Pleshanov S.A. *Quantum Electron*., **38**, 319 (2008) [*Kvantovaya Elektron*., **38**, 319 (2008)].
4. Ivanov A.V., Kurnosov V.D., Kurnosov K.V., Romantsevich V.I., Chernov R.V., Marmalyuk A.A., Volkov N.A., Zholnerov V.S. *Quantum Electron*., **41**, 692 (2011) [*Kvantovaya Elektron*., **41**, 692 (2011)].
5. Zholnerov V.S., Ivanov A.V., Kurnosov V.D., Kurnosov K.V., Lobintsov A.V., Romantsevich V.I., Chernov R.V. *Tech. Phys*., **57** (6), 797 (2012) [*Zh. Tekh. Fiz*., **82** (6), 63 (2012)].
6. Zholnerov V.S., Ivanov A.V., Kurnosov V.D., Kurnosov K.V., Romantsevich V.I., Chernov R.V. *Tech. Phys.*, **59** (3), 416 (2014) [*Zh. Tekh. Fiz*., **84** (3), 108 (2014)].
7. Timofeev F.N., Simin G.S., Shatalov M.S., Gurevich S.A., Bayvel P., Wyatt R., Lealman I., Kashyap R. *Fiber Integr. Opt*., **19**, 327 (2000).
8. Hisham H.K., Abas A.F., Mahdiraji G.A., Mahdi M.A., Mahamd Adikan F.R. *Opt. Eng*., **53**, 1 (2014).
9. Hisham H.K. *Open Phys. J*., **3**, 55 (2016).
10. Fang Z., Cai H., Chen G., Qu R. *Single Frequency Semiconductor Lasers* (Springer, 2017).
11. Wieman C.E., Holberg L. *Rev. Sci. Instrum*., **62**, 1 (1991).